Bulletin of the Seismological Society of America. Vol. 66, No. 1, pp. 153–171. February 1976

THE IDENTIFICATION OF BUILDING STRUCTURAL SYSTEMS
II. THE NONLINEAR CASE

BY P. Z. MARMARELIS AND F. E. UDWADIA

ABSTRACT

This paper models a building structure as a nonlinear feedback system and studies the effects of such a system model on the structural response to strong ground shaking. Nonlinear kernels arising in the identification procedure have been investigated and an error analysis presented.

Applications of the Weiner method in studying the response of a reinforced concrete structure to strong ground shaking have been illustrated. The nature of the second order kernels has been displayed and the nonlinear contribution to the response at the roof level, during strong ground shaking, has been determined.

INTRODUCTION

One has to contend with two main features in the analysis of structural systems subjected to strong ground shaking. First, as the earthquake motions progress, various parts of the structure may either be brought into action, or rendered out of action, so that the effective structural properties of the system (which provide the resistive forces to seismic loads) may change during the time history of ground motions. For example, many nonstructural elements, which, for sufficiently small ground motions may be capable of providing structural strength, may fail under larger, more severe, shaking. The system would then be described as being nonstationary in nature. Second, we have the added complexity that for these larger ground motions the system could behave in a nonlinear manner (even without undergoing structural deterioration). This nonlinear behavior could also, in part, be brought about by the deterioration that the structure undergoes during the ground shaking. For instance, one can conceive of a structure wherein the number of nonstructural elements which could perhaps be rendered out of action increases with the strain levels, so that the structure could exhibit a "soft spring" type nonlinearity.

The problem of system nonstationarity has been explored in part I of this study (Udwadia and Marmarelis, 1975) where a moving-window analysis was used to isolate segments during which the structural system remained almost time-invariant. As explained earlier (cf., part I), the general nonlinear technique which will be followed for the system identification requires this condition to be satisfied. Otherwise, the resulting characterization would be a "time-average" functional characterization of the system.

Although there is no *a priori* reason for representing building systems subjected to strong ground shaking by linear models, the linearity assumption is a widely accepted one (Nielsen, 1966). There are basically two reasons for this: first, the simplicity of the techniques involved and second, the near absence of powerful and general nonlinear system theories. Certain specialized methods for nonlinear system analysis exist such as the phase-plane and describing function techniques. However, all of these methods have serious limitations and are applicable to rather narrow classes of nonlinear systems. Starting with Wiener's original work in 1942 a general theory of nonlinear system analysis and synthesis has been in development (Wiener, 1958; Bose, 1956; Brilliant, 1958; George, 1958).

The theory is applicable to all systems that are time-invariant and have a finite memory and therefore covers a very wide range of physical systems.

In part I of this study we outlined Wiener's method and discussed its applicability to structural systems. It was pointed out that Wiener's technique of breaking the system down into a linear system followed by a memoryless nonlinear system resulted in the computation of a large number of coefficients and suffered from several disadvantages. The cross-correlation technique proposed by Lee and Schetzen (1965) has been used in this study. Besides being easily extensible to multi-input systems, the cross-correlation method has several advantages over the Wiener formulation and simplifies the identification problem in the following ways: (a) It directly estimates the kernels which, as it was described earlier, have a definite functional meaning; they can reveal interesting properties and provide an insight to the structure of the system under study. (b) The cross-correlation method is much simpler computationally because it does not involve the cumbersome Laguerre and Hermite transformations. (c) A linear system is easily recognized by the cross-corrleation method; the derived model takes a simple form and therefore the computational burden is reduced while the insight into the nature of the system is increased. (d) The synthesis problem is very simple. Estimating the response to a particular input involves only a few integrations. (e) It is very easy to construct alternative models once the kernels are known, such as structures consisting of linear filters (for which powerful theories exist) and multipliers. (f) In the Wiener formulation it can be considered that the kernels are expanded in terms of the orthogonal family of Laguerre functions, and since this expansion, for any practical application, has to be truncated, there is an inherent approximation error in the Wiener formulation. This truncation error does not occur in the cross-correlation method. (g) *a priori* information about the system can be utilized to reduce the identification effort by reducing the computational burden.

These cross-correlation techniques have so far been applied to determine the linear kernels characterizing the EW and NS response of a reinforced concrete structure. The performance of the linear model was evaluated (cf., part I) and it was noticed that the model performance was different in certain features from the measured response. Although some of these discrepancies are no doubt due to the fact that various assumptions underlying the method are not fully satisfied, it will be shown in this part that a good part of the discrepancies can be attributed to system nonlinearities.

The second-order nonlinear kernels of the system will be estimated and an examination of their contribution to the total system response carried out. The feedback model briefly outlined in part I has been extended to cover the nonlinear feedback case. Error analyses of the second-order kernels are presented and model responses synthesized. Mean-square error calculations have been done and the effect of the nonlinearity indicated. The resulting models, in terms of the linear kernel, $\{h_1(\tau), k_1(\tau)\}$, and the nonlinear kernel, $\{h_2(\tau_1, \tau_2), k_2(\tau_1, \tau_2)\}$, represent more accurate models as inferred from the computed and measured system responses during strong earthquake ground shaking.

Description of Nonlinearity in Terms of Wiener Kernels

It has been shown that, under large dynamic loads, structural systems exhibit marked nonlinear responses, often accompanied by a deteriorating behavior (Udwadia and Trifunac, 1973). Therefore, during the input-output measurement interval the system characteristics may not be time-invariant. However, the problem of time-variant nonlinear systems is generally unsolved. Here, we assume that the system is nonlinear but time-invariant over the time period during which the identification is carried out. This assumption is usually well justified. If not, the resulting characterization of the system is the average (in time) characterization (i.e., the nonlinear model exhibits the average characteristics). In part I, we described a procedure for determining how time-variant a building structural system is, utilizing a moving-window analysis. Based on the results of this procedure we choose two segments of record to be used for identification of the building structural system.

As discussed in part I, Wiener showed that the relationship between the input $x(t)$ and the output $y(t)$ of system S can be written as

$$y(t) = \sum_{n=0}^{\infty} G_n[h_n, x(t)] \tag{1}$$

where $\{G_i\}$ is a complete set of orthogonal functionals with respect to Gaussian white noise and $\{h_i\}$ is the set of kernels that characterize S.

Each h_k is a symmetric function with respect to its arguments. The first four Wiener functionals were represented in part I, and their functional relationships will not be repeated here.

The set of kernels $\{h_i\}$ can be considered to be the generalized "impulse responses" of system S. By considering the system response to inputs of single impulses applied at different times as well as the response to finite trains of impulses, it can easily be shown that the nonlinear kernels give a quantitative measure of the nonlinear "cross-talk" between different portions of the past input as it affects the present system response.

For example, for a system which has only a second-order nonlinearity, the characterizing kernel $h_2(t, t-t_\alpha)$ indicates the nonlinear interaction (for $t \geqq t_\alpha$) between the input at $t = 0$ and the input at $t = t_\alpha$ as it affects the system output at time t.

This can be shown as follows: Let S be a nonlinear system characterized by the input-output relationship

$$y(t) = \int_0^\infty h_1(\tau)x(t-\tau)d\tau + \iint_0^\infty h_2(\tau_1, \tau_2)x(t-\tau_1)x(t-\tau_2)d\tau_1 d\tau_2. \tag{2}$$

The response at time t due to an impulse at $t = 0$, i.e., for $x_1(t) = \delta(t)$ is

$$y_1(t) = h_1(t) + h_2(t, t).$$

Similarly, the response due to an impulse at $t = t_\alpha$, i.e., for $x_2(t) = \delta(t-t_\alpha)$, is

$$y_2(t) = h_1(t-t_\alpha) + h_2(t-t_\alpha, t-t_\alpha). \tag{3}$$

The response of the system S to a stimulus consisting of an impulse at time $t = 0$ and an impulse at time $t = t_\alpha$, i.e., for $x_3 = x_1 + x_2$, is

$$y_3(t) = h_1(t) + h_1(t-t_\alpha) + h_2(t, t) + 2h_2(t, t-t_\alpha) + h_2(t-t_\alpha, t-t_\alpha).$$

The difference in this response from that obtained by linear superposition, i.e.,

$$y_3(t) - [y_1(t) + y_2(t)] = 2h_2(t, t-t_\alpha), \tag{4}$$

represents the deviation of the second order, nonlinear system response from the linear, first-order representation.

The nonlinear kernels are found by use of cross-correlation techniques (Lee and Schetzen, 1965). For example, to estimate $h_2(\sigma_1, \sigma_2)$ we form the cross-correlation ($E\{\cdot\}$ means "expected value")

$$Q(\sigma_1, \sigma_2) = E\{[y(t) - \sum_0^1 G_n[h_n, x(t)]]x(t-\sigma_1)x(t-\sigma_2)\}$$

which, utilizing the orthogonality properties of the Wiener series and the fact that $x(t)$

is Gaussian white noise with zero mean [therefore $E\{x\} = 0$, $E\{x(t)x(t-\tau)\} = \phi_{xx}(\tau) = P\delta(\tau)$, $\phi_{xxx}(\tau_1, \tau_2) = 0$, etc.] gives

$$Q = E\{\iint h_2(\tau_1, \tau_2)x(t-\tau_1)x(t-\tau_2)d\tau_1 d\tau_2 \cdot x(t-\sigma_1)x(t-\sigma_2)\}$$
$$-E\{P \int h_2(\tau_1, \tau_1)d\tau_1 \cdot x(t-\sigma_1)x(t-\sigma_2)\}.$$

Next, considering that $x(t)$ is a Gaussian variable

$$\begin{aligned} E\{x(t-\tau_1)x(t-\tau_2)x(t-\sigma_1)x(t-\sigma_2)\} &= E\{x(t-\tau_1)x(t-\tau_2)\} \cdot E\{x(t-\sigma_1)x(t-\sigma_2)\} \\ &\quad + E\{x(t-\tau_1)x(t-\sigma_1)\} \cdot E\{x(t-\tau_2)x(t-\sigma_2)\} \\ &\quad + E\{x(t-\tau_1)x(t-\sigma_2)\} \cdot E\{x(t-\tau_2)x(t-\sigma_1)\} \\ &= \phi(\tau_1-\tau_2)\phi(\sigma_1-\sigma_2) + \phi(\tau_1-\sigma_1)\phi(\tau_2-\sigma_2) \\ &\quad + \phi(\tau_1-\sigma_2)\phi(\tau_2-\sigma_1) \end{aligned}$$

where $\phi(u)$ is the autocorrelation function of white noise $x(t)$, i.e., $\phi(u) = P\delta(u)$. Thus,

$$\begin{aligned} Q &= \delta(\sigma_1-\sigma_2) \iint_0^\infty h_2(\tau_1, \tau_2)\delta(\tau_1-\tau_2)d\tau_1 d\tau_2 \\ &\quad + P^2[h_2(\sigma_1, \sigma_2) + h_2(\sigma_2, \sigma_1)] \\ &\quad - P \int_0^\infty h_2(\tau_1, \tau_1)\phi(\sigma_1-\sigma_2)d\tau_1 \\ &= 2P^2 h_2(\sigma_1, \sigma_2) \end{aligned}$$

and therefore

$$h_2(\sigma_1, \sigma_2) = \frac{Q}{2P^2} = \frac{1}{2P^2} E\{[y(t) - \sum_0^1 G_n[h_n, x(t)]]x(t-\sigma_1)x(t-\sigma_2)\}. \tag{5}$$

Similarly, we have in general

$$h_n(\sigma_1, \sigma_2, \ldots, \sigma_n) = \frac{1}{n!P^n} E\{[y(t) - \sum_0^{n-1} G_m[h_m, x(t)]]x(t-\sigma_1)x(t-\sigma_2), \ldots, x(t-\sigma_n)\}. \tag{6}$$

Nonlinear Description of the Feedback Model

In part I we described briefly the feedback model of a building structural system. The transfer function of the system was derived assuming that each component is a linear subsystem. A similar analysis can be made even if each subsystem is nonlinear and described by a set of Wiener kernels.

Figure 1 shows the block diagram of a building whose component subsystems are B, R, and A. As discussed in part I, these components represent, respectively, the building element, the element which takes care of the reflection of signal when it reaches the boundary, and the feedback element (which is a composite of the elements B^*, L, T, and G). We shall assume for the sake of this discussion that the reflective element is linear while both B and A are nonlinear in nature. We assume that each subsystem can be described by the linear kernel $g_1(\tau)$ and the second-order nonlinear kernel $g_2(\tau_1, \tau_2)$, while the contribution of the higher-order kernels (g_3, g_4, etc.) is small. As discussed previously, the characterization of the system in terms of only $g_1(\tau)$ and $g_2(\tau_1, \tau_2)$ is the best second-order-nonlinear model of the system in the mean-square-error sense.

Brilliant (1958) has shown that any continuous, physically realizable system can be approximated arbitrarily closely in the form

$$y(t) = h_0+\int_0^\infty h_1(\tau)x(t-\tau)\,d\tau+\iint_0^\infty h_2(\tau_1,\tau_2)x(t-\tau_1)x(t-\tau_2)\,d\tau_1 d\tau_2$$
$$+\ldots+\iint_0^\infty\ldots\int h_n(\tau_1,\tau_2,\ldots,\tau_n)x(t-\tau_1)x(t-\tau_2)\ldots x(t-\tau_n)\,d\tau_1 d\tau_2\ldots d\tau_n \tag{7}$$

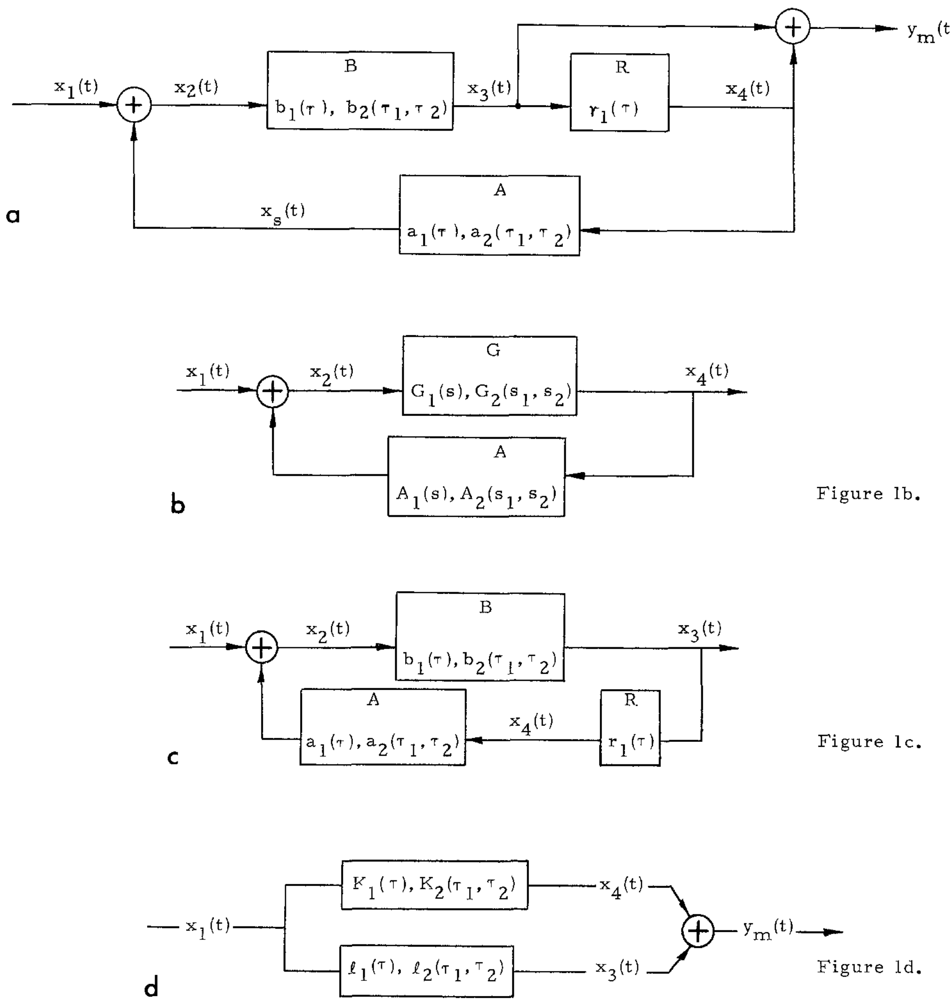

FIG. 1. Schematic black-box representation of the building-soil system, component B representing the building structure, and component A representing the feedback loop as described by nonlinear elements. Element R is the linear reflective element.

where $x(t)$ is the input and $y(t)$ is the output of the system. Without loss of generality, in the practical case, we can take h_0 to be zero (i.e., by measuring all variables from their values when the input is zero).

We should also note that

$$\int_0^\infty h_1(\tau)x(t-\tau)\,d\tau = \int_{-\infty}^\infty h_1(\tau)x(t-\tau)\,d\tau = \int_{-\infty}^\infty h_1(t-\tau)x(\tau)\,d\tau = \int_{-\infty}^t h_1(t-\tau)x(\tau)\,d\tau \tag{8}$$

since for physical systems $h_1(v) = 0$ for $v < 0$. A similar argument is valid for higher order kernels.

Let us consider now the cascade combination of systems B and R in Figure 1. We have

$$\begin{aligned} x_4(t) &= \int_{-\infty}^{\infty} r_1(t-\tau)x_3(\tau)d\tau \\ &= \int_{-\infty}^{\infty} r_1(t-\tau)[\int_{-\infty}^{\infty} b_1(\tau-\mu)x_2(\mu)d\mu \\ &\quad +\iint_{-\infty}^{\infty} b_2(\tau-\mu_1, \tau-\mu_2)x_2(\mu_1)x_2(\mu_2)d\mu_1 d\mu_2]\,d\tau \\ &= \int_{-\infty}^{\infty} [\int_{-\infty}^{\infty} r_1(t-\tau)b_1(t-\mu)d\tau]x_2(\mu)d\mu \\ &\quad +\iint_{-\infty}^{\infty} [\int_{-\infty}^{\infty} r_1(t-\tau)b_2(\tau-\mu_1, \tau-\mu_2)d\tau]x(\mu_1)x(\mu_2)d\mu_1 d\mu_2. \end{aligned} \tag{9}$$

Let us define the Laplace transforms of the system kernels by

$$\begin{aligned} H_1(s) &= \int_{-\infty}^{\infty} h_1(\tau)\exp(-s\tau)d\tau \\ H_2(s_1, s_2) &= \iint_{-\infty}^{\infty} h_2(\tau_1, \tau_2)\exp(-s_1\tau_1 - s_2\tau_2)d\tau_1 d\tau_2. \end{aligned} \tag{10}$$

Then, it is easily shown that the overall system kernels $g_1(\tau)$, $g_2(\tau_1, \tau_2)$ for the cascade combination of systems B and R have transforms

$$\begin{aligned} G_1(s) &= B_1(s)R_1(s) \\ G_2(s_1, s_2) &= R_1(s_1+s_2)B_2(s_1, s_2) \end{aligned} \tag{11}$$

where $B_1(s)$, $R_1(s)$, $B_2(s_1, s_2)$ are the transforms of kernels $b_1(\tau)$, $r_1(\tau)$ and $b_2(\tau_1, \tau_2)$, respectively.

Thus, now we have the situation shown in Figure 1b and we wish to find the kernels of the overall system which we call K. Let us denote by $y = S(x)$ the transformation of input x by system S to obtain the output y. Then we have

$$\begin{aligned} K(x_1) &= G(x_2) \\ &= G[x_1 + A(x_4)] \\ &= G\{x_1 + A[K(x_1)]\}. \end{aligned} \tag{12}$$

Note that since A, K, G are nonlinear systems, these operators do not necessarily commute. Let us call

$$\begin{aligned} Q(x_1) &= x_1 + A[K(x_1)] \\ &= I(x_1) + A[K(x_1)] \end{aligned}$$

where I is the identity system $[x = I(x)]$. We note that $A[K(x_1)]$ denotes the cascade combination of system K followed by system A. Such a cascade combination was described above. It can then be shown easily that (Brilliant, 1958; Barrett, 1963)

$$\begin{aligned} Q_1(s) &= 1 + A_1(s)K_1(s) \\ Q_2(s_1, s_2) &= A_1(s_1+s_2)K_2(s_1, s_2) + A_2(s_1, s_2)K_1(s_1)K_1(s_2). \end{aligned} \tag{13}$$

A similar expression can be derived for $Q_3(s_1, s_2, s_3)$, etc. But then, $K(x_1) = G[Q(x_1)]$ which is again a cascade of system Q followed by system G. Thus, we finally get

$$K_1(s) = \frac{G_1(s)}{1 - G_1(s)A_1(s)} = \frac{B_1(s)R_1(s)}{1 - B_1(s)R_1(s)A_1(s)}$$

$$K_2(s_1, s_2) = \frac{G_1(s_1)G_1(s_2)G_1(s_1+s_2)A_2(s_1, s_2) + G_2(s_1, s_2)}{[1 - G_1(s_1)A_1(s_1)][1 - G_1(s_2)A_1(s_2)][1 - G_1(s_1+s_2)A_1(s_1+s_2)]}$$

$$= \frac{B_1(s_1)R_1(s_1)B_1(s_2)B_1(s_1+s_2)R_1(s_1+s_2)A_2(s_1, s_2)+R_1(s_1+s_2)B_2(s_1, s_2)}{[1-B_1(s_1)R_1(s_1)A_1(s_1)][1-B_1(s_2)R_1(s_2)A_1(s_2)][1-B_1(s_1+s_2)R_1(s_1+s_2)A_1(s_1+s_2)]}. \tag{14}$$

A similar expression can be derived for $K_3(s_1, s_2, s_3)$, etc.

In order to find the transfer functional of signal $x_1(t)$ to $y_m(t)$, we need to find the transfer functional of $x_1(t)$ to $x_3(t)$, in addition to that of $x_1(t)$ to $x_4(t)$ which was found in the previous paragraph. Now we have the situation shown in Figure 1c.

Proceeding similarly, as above, we find that the kernels of this system are given by

$$L_1(s) = \frac{B_1(s)}{1-B_1(s)R_1(s)A_1(s)}$$

$$L_2(s_1, s_2) =$$

$$\frac{B_1(s_1)B_1(s_2)B_1(s_1+s_2)R_1(s_1)R_1(s_2)A_2(s_1, s_2)+B_2(s_1, s_2)}{[1-B_1(s_1)R_1(s_1)A_1(s_1)][1-B_1(s_2)R_1(s_2)A_1(s_2)][1-B_1(s_1+s_2)A_1(s_1+s_2)R_1(s+s_2)]}. \tag{15}$$

Since $y_m(t)$ is the sum of $x_3(t)$ and $x_4(t)$, it can be represented as shown in Figure 1d. It then follows now that the kernels of the overall transfer functional $x_1(t)$ to the measured response $y_m(t)$ are given by

$$H_1(s) = K_1(s)+L_1(s) = \frac{B_1(s)[1+R_1(s)]}{1-B_1(s)R_1(s)A_1(s)}$$

$$H_2(s_1, s_2) = K_2(s_1, s_2)+L_2(s_1, s_2)$$

$$= \frac{[B_1(s_1)R_1(s_1)B_1(s_2)R_1(s_2)B_1(s_1+s_2)A_2(s_1, s_2)+B_2(s_1, s_2)][1+R_1(s_1+s_2)]}{[1-B_1(s_1)A_1(s_1)R_1(s_1)][1-B_1(s_2)A_1(s_2)R_1(s_2)][1-B_1(s_1+s_2)A_1(s_1+s_2)R_1(s_1+s_2)]}. \tag{16}$$

Similar expressions, but algebraically more complex, can be derived for $H_3(s_1, s_2, s_3)$, etc.

It is noted that the kernel transforms of a system which is a combination of subsystems are given in terms of algebraic equations which involve linearly the transforms of the kernels of the subsystems, as would be expcted. However, the expressions tend to increase rapidly in complication as the order of the kernel is increased. In principle, these equations can be solved in the frequency domain for any of the kernel transforms and then inverted back to the time domain, resulting in the system kernels $h_1(\tau)$, $h_2(\tau_1, \tau_2)$, etc.

From equation (16) it is noted that the poles of $H_1(s)$ *and* $H_2(s_1, s_2)$ both are given by the zeros, f_0, of the expression

$$1-B_1(u)A_1(u)R_1(u) = 0. \tag{17}$$

This signifies that kernels $h_1(\tau)$ and $h_2(\tau_1, \tau_2)$ have "resonance" peaks at the same frequencies f_0. However, kernel $h_2(\tau_1, \tau_2)$ has, in addition, resonance peaks for frequencies (s_1, s_2) whose sum equals f_0, as indicated by the factor

$$1-B_1(s_1+s_2)A_1(s_1+s_2)R_1(s_1+s_2) = 0 \tag{18}$$

in equation (16).

Error Analysis for Nonlinear Kernels

As discussed in part I, nonlincarities in structural responses depend closely on the amplitude range and frequency content of the exciting source. Since we are interested in the earthquake response of structures, we wish to conduct tests with input amplitudes comparable to those caused by earthquakes. However, the generation of white inputs at such large dynamic loads is extremely difficult. Therefore, we are forced to revert to naturally occurring loads such as those caused by an earthquake. However, we cannot expect these loads to be generally white in frequency content and therefore we need to analyze the effect of the nonwhiteness of the inputs on the estimation of the kernels. To this end, let us assume that the nonwhite input $\tilde{x}(t)$ is produced after a white input $x(t)$ passes through a linear filter with impulse response $l(\tau)$. Then,

$$\tilde{x}(t) = \int l(v)x(t-v)\,dv$$

and the second order (nonlinear) kernel is estimated by taking

$$\hat{h}_2(\tau_1, \tau_2) = C_2\phi_{y\tilde{x}\tilde{x}}(\tau_1, \tau_2) = C_2 E[y(t)\tilde{x}(t-\tau_1)\tilde{x}(t-\tau_2)]$$

where $C_2 = 1/2P^2$ if the noise is white, i.e., $\phi_{\tilde{x}\tilde{x}}(u) = P\delta(u)$. We have,

$$\phi_{y\tilde{x}\tilde{x}}(\tau_1, \tau_2) = E[y(t)\int_0^\infty l(\alpha_1)x(t-\tau_1-\alpha_1)d\alpha_1 \cdot \int_0^\infty l(\alpha_2)x(t-\tau_2-\alpha_2)\,d\alpha_2]$$

which becomes

$$\phi_{y\tilde{x}\tilde{x}}(\tau_1, \tau_2) = \iint_0^\infty l(\alpha_1)l(\alpha_2)\phi_{yxx}(\tau_1+\alpha_1, \tau_2+\alpha_2)\,d\alpha_1 d\alpha_2 .$$

Taking transforms on either side we have

$$H_2(\omega_1, \omega_2) = \frac{\hat{H}_2(\omega_1, \omega_2)}{\bar{L}(\omega_1)\bar{L}(\omega_2)} \tag{19}$$

where $L(\omega)$ is the Fourier transform of $l(\tau)$ [$\bar{L}(\omega)$ is its complex conjugate] and $H_2(\omega_1, \omega_2)$ and $\hat{H}_2(\omega_1, \omega_2)$ are the two-dimensional transforms of $h_2(\tau_1, \tau_2)$ and $\hat{h}_2(\tau_1, \tau_2)$. From equation (12) it is observed that for $\hat{h}_2(\tau_1, \tau_2)$ to be a good estimate of $h_2(\tau_1, \tau_2)$, all that is required is that the system bandwidth be completely covered by the input signal bandwidth. For large ω's the gain of the low-pass filter $l(\tau)$ will be substantially different from 1 and large errors may arise in computing $h_2(\tau_1, \tau_2)$ there. We conclude that the bandwidth of the input noise should be greater than the system bandwidth. This provides the lower bound for the test noise bandwidth. However, if this bandwidth extends too much beyond the system bandwidth, the statistical variance of the kernel estimates increases considerably. This can be shown by an analysis similar to that of part I for the first-order kernel. This analysis determines the upper bound of the input signal bandwidth.

For example, if the system is nonlinear with $h_0 \neq 0$, $h_1(\tau) \neq 0$, $h_2(\tau_1, \tau_2) \neq 0$ and $h_n(\tau_1, \tau_2, \ldots, \tau_n) = 0$ for $n \geqq 3$, it can be shown (Marmarelis and Naka, 1974) that the nonlinearity (i.e., h_2) contributes an additional term to the variance of the $h_1(\tau)$ estimate which is given by equation (19) (part I). This term is

$$\iiiint_0^\infty h_2(v_1, v_2)h_2(\mu_1, \mu_2)[\sum \Pi E\{x_i x_j\}]\,dv_1 dv_2 d\mu_1 d\mu_2$$

where $\Sigma\Pi$ means the sum of all distinct ways of partitioning $x(t-\tau)x(t-\tau)x(t-v_1)$ $x(t-v_2)\ldots$ into pairs. There will be $6!/3!2^3 = 15$ terms, such as

$$\phi_{xx}(0)\phi_{xx}(v_1-v_2)\phi_{xx}(\mu_1-\mu_2) + \phi_{xx}(\tau-v_1)\phi_{xx}(\tau-v_2)\phi_{xx}(\mu_1-\mu_2) + \ldots$$

where Q_{xx} is the autocorrelation function of $x(t)$. These terms can, similarly, as in part I, be expressed in terms of their (multidimensional) Fourier transforms.

The effect of random (contaminating noise) distributed loads on the nonlinear kernel estimation can be analyzed similarly as in part I for the linear case. Assuming that these unwanted "noise" inputs γ_i follow a different path through the system than the "input" noise signal x, we have

$$y(t) = \sum_n G_n[h_n, x(t)] + \sum_i \sum_m \{H_m[K_{mi}, \gamma_i(t)]\}.$$

It can be shown then that if $m = 1$

$$\hat{h}_n(\tau_1, \tau_2, \ldots, \tau_n) = h_n(\tau_1, \tau_2, \ldots, \tau_n) + \sum \int K_{1_i}(v)\phi_{x \ldots x\gamma_i}(v-\tau_1, \ldots, v-\tau_n)dv.$$

It should be noted that the contributions to the error of nonlinearities other than of the nth order is zero because their corresponding functionals would be orthogonal with respect to a Gaussian white $x(t)$. In fact, if $x(t)$ and $\gamma_i(t)$ are independent, then the error term becomes zero at least for odd-order kernels and, in addition, for even-order ones if $E\{\gamma_i\} = 0$. Thus, a great advantage is gained in the determination of the system transfer characteristic by this approach as compared to the more traditional methods of testing the system with pulses and sinewaves. Provided that the contaminating noise is independent of the stimulating white-noise signal, the presence of such noise does not affect the estimation of the characterizing kernels.

Measurement noise $\varepsilon(t)$, which is simply additive at the output, can be similarly treated, giving

$$\hat{h}_n(\tau_1, \ldots, \tau_n) = h_n(\tau_1, \ldots, \tau_n) + \frac{1}{n!P^n}\phi_{x \ldots x\varepsilon}(\tau_1, \ldots, \tau_n).$$

Unwanted noise, which is additive at the input, other than measurement noise tends to be more serious in the measurement of the nonlinear kernels and the number of error terms increases rapidly with the order of the computed kernel and with the order of nonlinearity of the system. This should be contrasted with the case of errors at the output which, as seen previously, do not increase as either of these orders are increased.

Application to a Reinforced Concrete Structure

In part I of this study we described the building structure to which the method was applied, the procedure for selecting the record lengths, and the data processing techniques utilized. The linear Wiener kernels were also estimated and their performance in studying the building response was evaluated. In this part, we present the results of estimating the nonlinear second-order kernels and of evaluating their performance (in a quantitative manner) in modeling the building response during strong earthquake ground shaking.

These second-order kernels were computed up to 2 sec (due to limitations of computer storage), following the cross-correlation techniques discussed in part I of this study. They have been referred to as $h_2(\tau_1, \tau_2)$ and $k_2(\tau_1, \tau_2)$ for the [3–43]-sec and [43–83]-sec EW time windows and $m_2(\tau_1, \tau_2)$ and $n_2(\tau_1, \tau_2)$ for the [3–43]- and [43–83]-sec NS time windows. Figures 2, 3, 4, and 5 show contours of the h_2, k_2, m_2, and n_2 surfaces (normalized with respect to each other) on which the kernels have constant "strength." The symmetry of the kernels may be observed, as expected. These kernels show clearly the nonlinear character of the system insofar as its response differs from linear superposition. As discussed previously, these kernel figures and tables can be interpreted to signify the following about the system's nonlinear behavior: Assuming that the system can be accurately represented by the first two kernels, the value of $h_2(t, t-t_0)$ quantizes the deviation in the system response at time $t \geqq t_0$ from linear superposition of the responses to two impulse inputs, one at time $t = 0$ and the other at time $t = t_0$. In short, it is the deviation from superposition due to cross-talk between portions of the past input.

Comparing the h_2 and k_2 kernels, we observe that the nature of the nonlinearity corresponding to the two time windows is different. The h_2 kernel is more or less concentrated in bands which lie along the diagonal line ($\tau_1 = \tau_2$), the contours of h_2 showing a marked elongated character, the elongation being in the direction of the diagonal. The contours of the k_2 kernel do not show such a markedly "directional" character. However, the general features of the two kernels are similar as we go down along the $\tau_1 = \tau_2$ line (compare crests and valleys). The extent of nonlinearity, as indicated by the values of the contours of h_2 and k_2, indicates that the structure showed a marked second-order

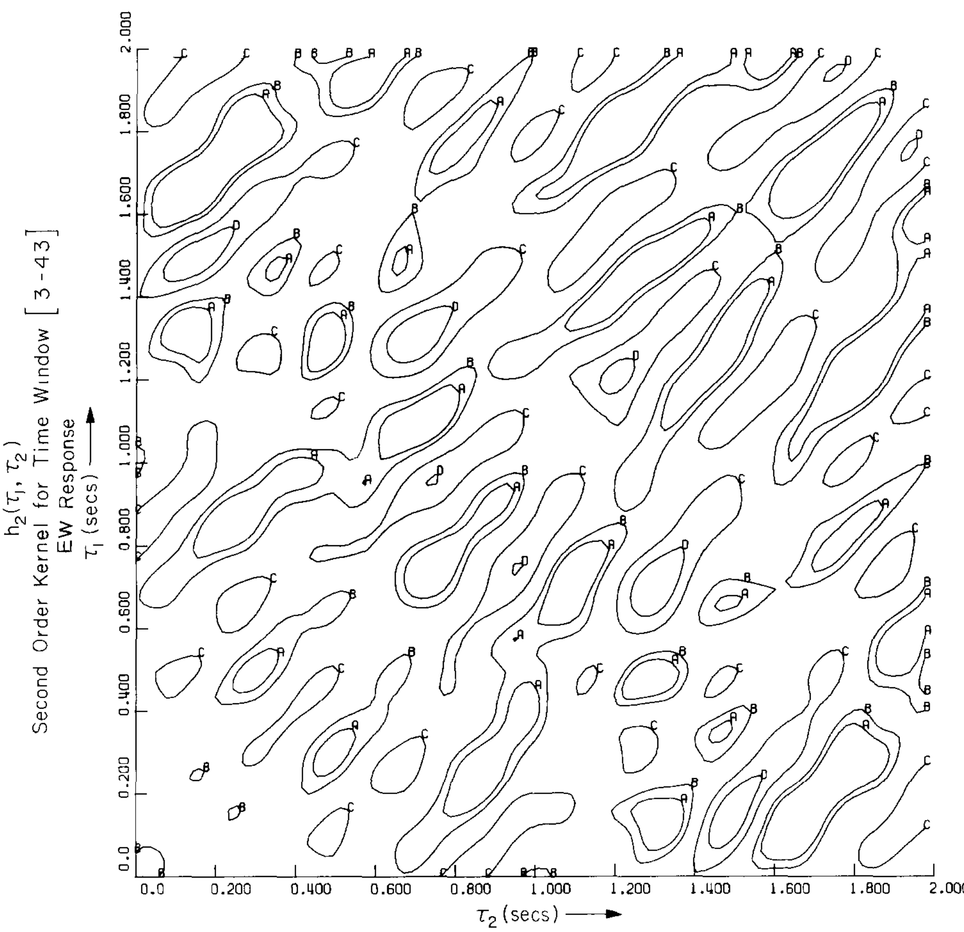

FIG. 2. Contour plot of kernel $h_2(\tau_1, \tau_2)$ corresponding to the EW time window [3–43] sec. The contour values are: $A = -125$, $B = -75$, $C = 100$, $D = 200$.

nonlinearity during the first 40 sec or so of excitation in the EW direction. It may be noted that when all the contour values tend to zero (or are very small), the second-order nonlinearity would vanish (or be very small). The normalized values of these kernels have been indicated in Tables 1 and 2, where the matrices have been normalized and displayed at time intervals 3/50 sec along the τ_1 and τ_2 axes. The h_2 kernel has been scaled by a factor of 5 for ease of representation. The actual computations involved the determination of these matrices at intervals of 1/50 sec.

The $m_2(\tau_1, \tau_2)$ and $n_2(\tau_1, \tau_2)$ kernels for the NS time window are displayed in Figures 4 and 5. The $m_2(\tau_1, \tau_2)$ kernel shows features similar to those depicted by the $h_2(\tau_1, \tau_2)$

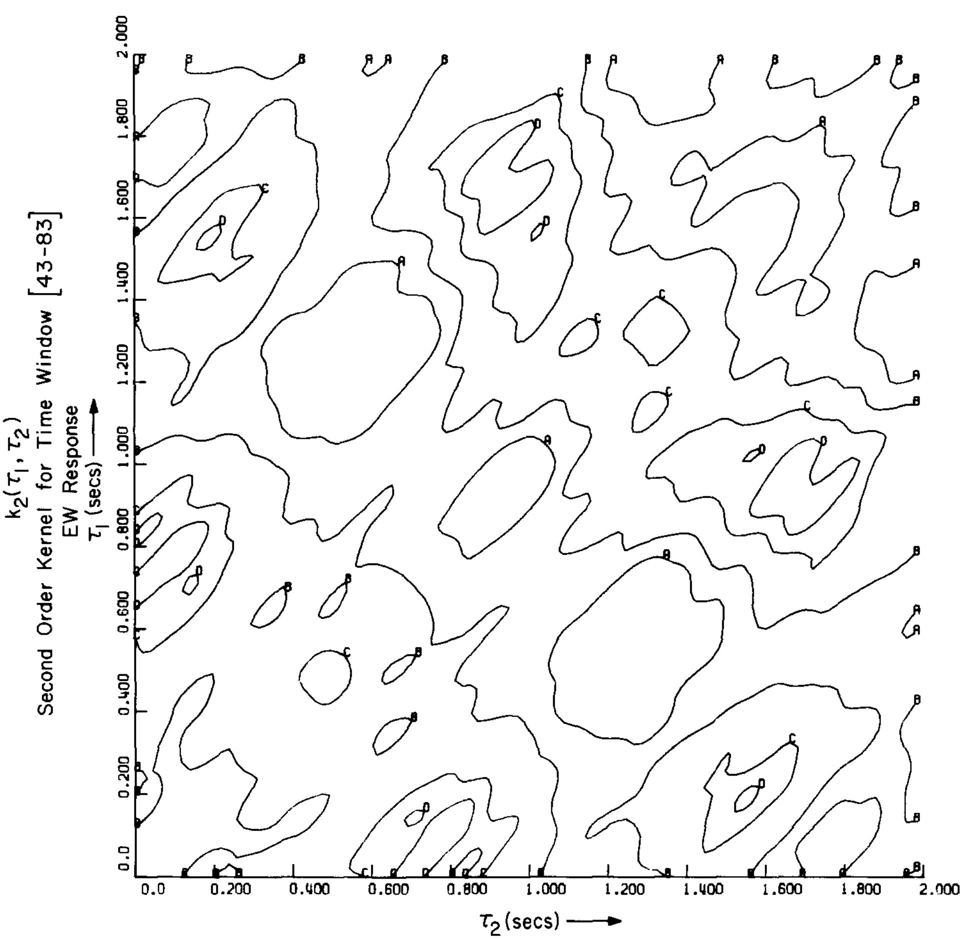

FIG. 3. Contour plot of kernel $k_2(\tau_1, \tau_2)$ corresponding to the EW time window [43–83] sec. The contour values are $A = -15$, $B = 0$, $C = 15$, $D = 25$.

TABLE 1

SECOND ORDER KERNEL $h_2(\tau_1, \tau_2)$

Time Window [3-43]
Component East

τ_2 (secs) ↓ \ τ_1 (secs) →	0	6	12	18	24	30	36	42	48	54	60	66	72	78	84	90	96	102	108	114	120	126	132	138	144	150	156	162	168	174	180	186	192	198
0	-20																																	
6	-15	-16																																
12	-3	-3	4																															
18	6	4	-1	0																														
24	0	-2	-12	-13	6																													
30	-4	-7	-10	-7	8	25																												
36	-7	C	-6	-5	7	12	23																											
42	-4	13	8	-12	-14	-11	7	26																										
48	15	22	27	4	-23	-32	-14	13	27																									
54	17	13	18	18	-2	-25	-26	-6	10	13																								
60	5	2	1	12	22	4	-19	-16	-11	2	4																							
66	-11	-16	-5	14	32	29	-1	-11	-21	-13	2	-9																						
72	-5	-23	-19	2	16	25	17	9	1	-7	-5	-16	-41																					
78	22	-4	-21	-24	-13	-3	11	18	22	20	11	-10	-33	-47																				
84	24	22	-8	-34	-40	-24	0	11	13	11	20	12	-3	-16	-29																			
90	18	27	18	-14	-37	-34	-18	-9	-5	-15	0	25	24	13	-15	-31																		
96	-9	12	30	22	-8	-23	-31	-29	-21	-20	-22	10	37	37	9	-16	-24																	
102	-19	-2	18	28	6	-6	-19	-27	-22	-15	-23	-22	1	26	30	20	6	2																
108	-11	-3	17	27	6	-7	0	6	4	-7	-20	-36	-43	-19	16	29	26	6	0															
114	-1	1	2	11	5	-2	3	14	23	11	-10	-23	-39	-42	-9	11	19	9	3	14														
120	-4	7	-7	-9	9	8	13	-9	3	13	11	10	2	-22	-19	-12	-10	4	17	27	48													
126	-10	-14	-21	-23	14	29	23	-16	-37	-6	23	42	39	11	-12	-15	-23	-20	2	16	31	40												
132	2	-24	-37	-29	-3	19	17	-12	-38	-20	18	48	59	37	8	-4	-11	-17	-24	-17	-4	18	26											
138	18	-2	-27	-26	-9	-1	0	-1	-22	-15	-2	15	35	44	29	14	3	7	-8	32	-32	-7	18	36										
144	17	32	27	5	-11	-17	-20	14	13	2	-11	-19	-4	14	32	30	15	14	25	-2	-35	-34	-14	15	34									
150	0	28	57	50	14	-12	-28	-4	24	14	-5	-27	-17	-4	15	28	24	14	28	32	-4	-35	-39	-27	5	9								
156	-10	-13	15	42	41	14	-7	-14	6	13	2	-19	-14	4	6	9	9	5	9	33	31	2	-20	-36	-28	-8	-5							
162	-7	-34	-39	-17	26	34	18	1	0	5	12	-5	-13	4	5	-2	-15	-16	-9	12	33	30	16	0	-19	-17	-16	-27						
168	-5	-32	-51	-44	-11	23	25	16	13	7	16	7	-19	-12	-7	4	-7	-24	-27	-12	12	27	27	17	7	-1	-11	-28	-49					
174	2	-4	-24	-42	-45	-19	4	20	27	19	12	16	-13	-30	-20	-1	20	4	-18	-35	-29	-10	12	16	19	27	11	-12	-37	-51				
180	10	14	11	-15	-50	-48	-28	-4	12	18	9	15	8	-22	-30	-13	19	27	3	-32	-54	-42	-10	12	15	26	32	16	-1	-29	-44			
186	15	26	16	-1	-31	-40	-21	-11	-15	-17	-6	14	27	12	-19	-28	-2	19	19	-7	-44	-56	-35	1	12	6	16	24	25	11	-21	-32		
192	5	24	31	14	-5	-21	-13	-8	-22	-41	-32	0	25	30	13	-16	-18	3	16	19	-3	-25	-42	-29	-11	-11	-16	-2	27	37	20	-9	-15	
198	-13	4	28	37	26	6	-9	-17	-16	-29	-35	-24	3	16	19	10	-14	-11	11	26	21	6	-15	-32	-31	-25	-28	-34	-2	33	40	22	1	-6

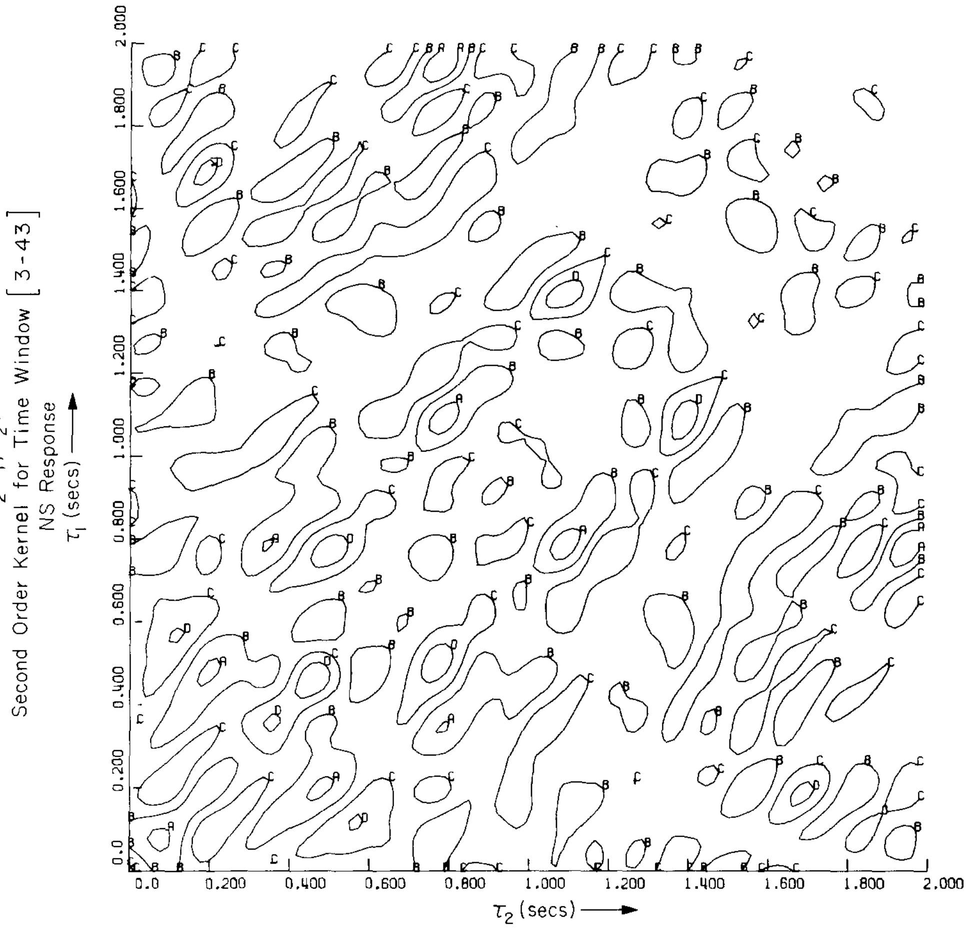

FIG. 4. Contour plot of kernel $m_2(\tau_1, \tau_2)$ corresponding to the NS time window [3–43] sec. The contour values are $A = -120$, $B = -50$, $C = 50$, $D = 150$.

TABLE 2

SECOND ORDER KERNEL $k_2(\tau_1, \tau_2)$

Time Window [43-83]
Component East

τ_2 (secs) ↓ \ τ_1 (secs) →	0	6	12	18	24	30	36	42	48	54	60	66	72	78	84	90	96	102	108	114	120	126	132	138	144	150	156	162	168	174	180	186	192	198
0	-4																																	
6	-10	-9																																
12	0	-12	-7																															
18	4	-1	-7	-1																														
24	-3	0	-2	-4	-3																													
30	6	-1	0	3	-1	6																												
36	7	4	-1	4	3	3	6																											
42	6	6	-2	0	5	2	6	11																										
48	11	5	5	-1	5	3	7	15	19																									
54	14	11	3	6	2	5	4	8	17	15																								
60	16	19	13	8	7	1	5	3	5	11	11																							
66	26	18	23	13	8	4	-3	5	0	4	11	8																						
72	28	28	24	23	8	6	2	3	5	0	4	4	-1																					
78	23	27	31	22	16	5	3	3	5	3	-1	-3	-6	-7																				
84	25	23	29	27	14	11	2	4	-1	1	-2	-10	-9	-15	-17																			
90	13	24	18	17	16	8	4	-4	-2	-4	1	-4	-10	-10	-20	-23																		
96	10	10	18	8	5	6	4	-5	-9	-5	-7	0	-9	-7	-12	-24	-18																	
102	2	7	7	10	5	1	-1	-5	-13	-9	-5	-8	-4	-9	-6	-14	-22	-17																
108	-3	-2	0	-2	1	-3	-10	-17	-15	-17	-11	-8	-10	-1	-5	-4	-8	-15	-10															
114	-9	-2	-3	-9	-8	-8	-14	-26	-29	-22	-22	-10	-11	-6	7	-2	6	2	-5	7														
120	-12	-7	1	-6	-11	-10	-19	-24	-31	-32	-24	-23	-9	-5	4	8	3	11	6	6	12													
126	-5	-5	-2	0	-8	-13	-17	-30	-26	-32	-35	-26	-23	-4	1	7	10	9	13	11	9	10												
132	-3	3	4	3	1	-7	-18	-20	-33	-29	-34	-32	-24	-15	4	6	13	14	11	19	14	15	20											
138	3	6	6	9	4	2	-9	-15	-20	-34	-28	-27	-25	-13	1	13	15	19	12	13	13	12	17	17										
144	5	14	12	13	12	6	0	-7	-11	-22	-30	-18	-11	-7	1	12	18	19	17	10	11	8	11	12	7									
150	4	12	20	18	15	14	6	-4	-5	-12	-16	-17	-6	4	11	14	19	19	17	12	3	6	3	4	6	2								
156	2	7	15	27	19	12	11	2	-7	-7	-7	-4	-4	2	16	23	21	25	18	14	5	-4	-1	-7	-7	-2	-3							
162	-7	0	8	17	22	13	9	6	-2	-9	-2	6	4	10	15	29	28	22	23	10	8	0	-6	-4	-17	-12	-8	-9						
168	-10	-13	1	10	15	17	11	6	-1	-3	-8	6	12	12	26	27	33	30	22	15	1	0	-8	-13	-12	-20	-15	-13	-14					
174	-22	-18	-16	-2	6	8	11	6	0	-3	-2	0	12	15	20	33	25	26	24	14	5	-9	-7	-14	-17	-16	-23	-20	-19	-19				
180	-17	-24	-18	-15	-3	2	5	2	-1	-2	-5	-1	3	11	18	21	32	21	19	11	1	-6	-11	-8	-13	-9	-11	-19	-16	-19	-11			
186	-11	-16	-21	-15	-11	0	5	-1	-8	-5	-4	-4	1	3	8	15	17	25	17	6	0	-9	-16	-16	-14	-10	-3	-7	-7	-11	-12	-6		
192	-12	-10	-11	-14	-13	-6	-2	-2	-7	-13	-10	-3	-2	5	7	8	12	12	16	2	-11	-14	-19	-22	-18	-14	-7	-2	-4	0	-4	-6	-4	
198	1	-9	-1	1	-1	0	2	-2	-5	-8	-16	-8	-2	1	7	10	10	9	9	4	-11	-24	-30	-28	-25	-11	-5	-2	7	1	9	4	-4	6

kernel. However, the kernel strengths show that the numerical values of the $m_2(\tau_1, \tau_2)$ kernel are (on an average) about one-half as large as those of the $h_2(\tau_1, \tau_2)$ kernel, indicating that the structure portrayed larger nonlinear effects in the EW than in the NS direction. This appears reasonable as the shear walls in the NS direction provide a great deal of structural stiffness in resisting lateral loads. In the EW direction, however, the horizontal loads are supported solely by the central core wall (Figure 2, part I) and the structural framework. The $n_2(\tau_1, \tau_2)$ kernel surface has amplitudes less than those of the $m_2(\tau_1, \tau_2)$ and shows a more lumpy contour character in contrast with the linear

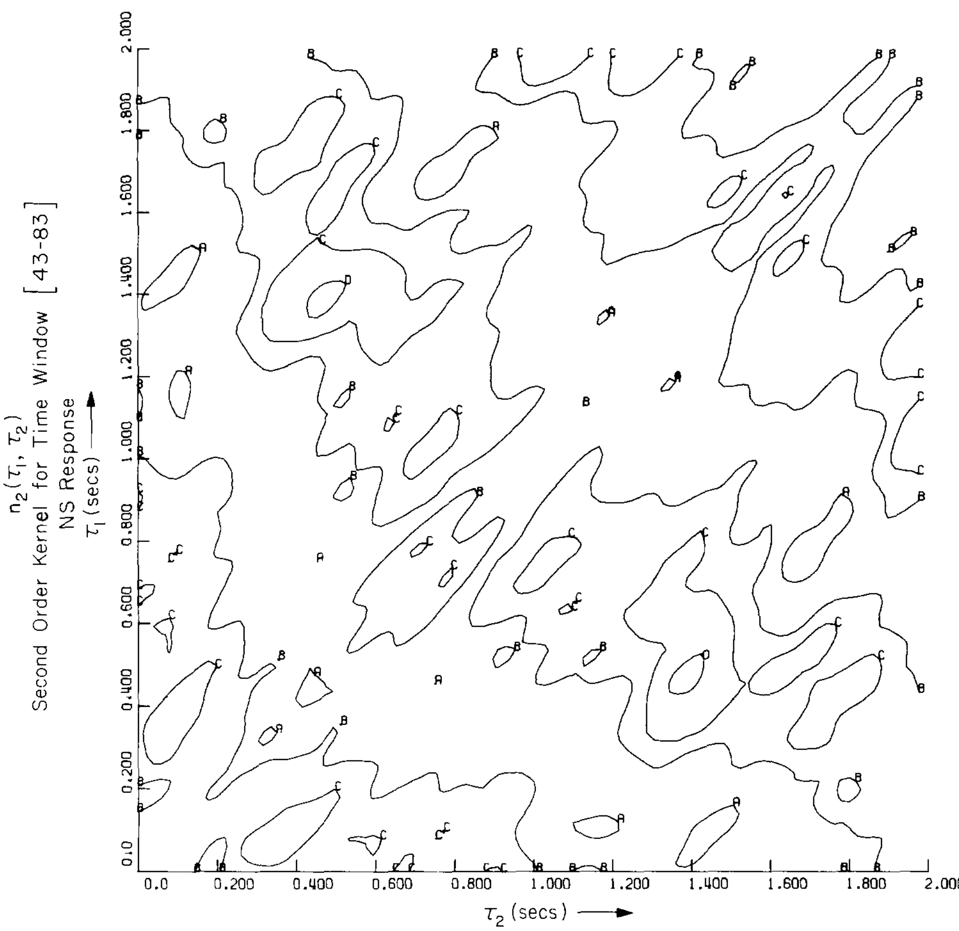

FIG. 5. Contour plot of kernel $n_2(\tau_1, \tau_2)$ corresponding to the NS time window [43–83] sec. The contour values are $A = -15$, $B = 0$, $C = 10$, $D = 20$.

elongated contour character of the $m_2(\tau_1, \tau_2)$ kernel. It is interesting to note that although the extent of nonlinearity in the EW and NS directions are different, the nature of the changes in the nonlinear kernels, as computed for the two time windows, in the EW and NS directions are rather similar. The normalized $m_2(\tau_1, \tau_2)$ and $n_2(\tau_1, \tau_2)$ matrices are displayed in Tables 3 and 4. The $m_2(\tau_1, \tau_2)$ kernel has been scaled by a factor of 5 for ease of presentation.

Thus, having identified the linear and nonlinear kernels of the structural systems, the predicted response of the model (linear and nonlinear) was computed. The linear response obtained from $G_1[h_1(t); x(\tau)]$ was determined and then the nonlinear contribution

$G_2[h_2(t); x(\tau)]$. A comparison with the actual measured response was made to determine the validity of the nonlinear model characterization.

It is of importance to discuss here how the nonlinear kernels were weighted against the linear ones, since the input signal (earthquake) deviates from true bandlimited white

TABLE 3

SECOND ORDER KERNEL $m_2(\tau_1, \tau_2)$

τ_1 (secs) →

Time Window [3-43]
Component North

← τ_2 (secs)	0	6	12	18	24	30	36	42	48	54	60	66	72	78	84	90	96	102	108	114	120	126	132	138	144	150	156	162	168	174	180	186	192	198
0	14																																	
6	-10	-30																																
12	-11	-20	-22																															
18	6	20	8	-25																														
24	8	9	20	-3	-19																													
30	7	-11	4	15	0	3																												
36	8	-2	-23	-2	9	15	33																											
42	-1	9	-16	-23	-2	-2	8	29																										
48	0	16	2	-31	-24	-12	-14	19	45																									
54	2	17	25	-10	-23	-8	-8	-6	4	-5																								
60	-4	12	28	18	0	-6	-4	-11	-22	-12	7																							
66	-3	9	10	11	7	-1	6	0	-8	-10	-7	-4																						
72	-10	-10	-3	10	5	-11	4	17	20	5	-8	-5	-8																					
78	-15	-24	-16	14	7	-18	-28	4	36	35	6	-4	-13	-23																				
84	10	-5	-17	-4	0	-4	-22	-18	2	18	10	5	3	0	2																			
90	16	0	5	-2	-4	2	-1	-14	-22	-7	14	13	6	12	5	-12																		
96	0	3	11	18	13	7	-9	-14	-9	2	0	-7	-3	14	9	-2	-9																	
102	-7	-3	6	9	11	15	17	-13	-19	-4	-1	-6	-9	-4	8	7	5	10																
108	-9	-11	-10	-9	-6	4	22	11	-11	-3	16	19	-5	-37	-16	6	11	6	0															
114	4	2	-14	-16	-8	-3	-2	12	9	5	8	16	11	-19	-28	-10	1	-2	-2	0														
120	9	10	3	-11	-5	3	-4	-8	0	-2	-7	-3	16	28	-5	-24	-13	-1	5	5	-1													
126	-9	-8	3	8	7	-2	-13	-10	-5	-2	-5	-4	5	17	9	6	6	-5	-15	-11	2	23												
132	5	-7	-1	4	5	5	-9	-5	2	-4	-12	-11	0	3	6	12	13	1	-10	-4	3	9	8											
138	19	14	2	-4	-3	5	17	11	-6	-18	-16	-11	-1	13	5	-12	-16	12	36	22	-5	-15	-13	-11										
144	-4	12	0	4	10	-2	-8	8	16	3	-6	-4	-6	-3	7	3	-19	-13	20	29	4	-14	-10	-6	-6									
150	-26	-2	-6	-7	9	4	-4	-5	3	11	11	10	8	-3	-2	7	-2	-18	-16	-1	10	0	-2	4	5	2								
156	-6	-8	-2	-26	-15	14	24	8	-17	-13	8	12	13	16	-2	-18	-1	0	-8	-10	-3	4	9	7	9	-2	-22							
162	14	-4	10	-4	-16	-6	-3	10	6	-14	-3	-1	-4	12	15	-5	1	4	3	-1	-6	-3	3	2	4	-6	-19	-11						
168	10	-5	7	33	8	-8	-19	-21	10	13	-12	-10	-15	-4	20	19	1	9	3	6	2	0	-13	-17	-14	4	7	8	3					
174	2	-4	-13	21	20	-1	4	-11	-16	8	5	1	-2	-15	0	15	-8	-5	6	3	-1	9	-7	-7	-12	6	14	3	-10	5				
180	-5	6	-9	-15	-2	-2	8	13	-3	-2	7	-1	11	1	-10	0	-4	-21	-12	-5	1	1	2	10	6	-7	7	5	-5	3	4			
186	-3	13	12	-19	-15	-3	5	11	8	2	1	-17	-1	28	2	-16	5	-4	-14	-7	4	-6	-3	9	14	-13	-12	6	7	-1	5	10		
192	0	-13	3	10	-2	-5	-1	6	10	7	10	7	-20	-22	7	1	7	9	-16	-14	8	7	0	0	2	3	-4	-4	6	-1	1	9	1	
198	-8	-14	-7	18	16	3	-8	3	4	2	4	20	0	-44	-22	21	13	8	-7	-20	0	18	8	-11	-10	3	11	-1	1	5	-1	-5	1	4

TABLE 4

SECOND ORDER KERNEL $n_2(\tau_1, \tau_2)$

τ_1 (secs) →

Time Window [43-83]
Component North

← τ_2 (secs)	0	6	12	18	24	30	36	42	48	54	60	66	72	78	84	90	96	102	108	114	120	126	132	138	144	150	156	162	168	174	180	186	192	198
0	7																																	
6	0	9																																
12	5	9	8																															
18	-4	0	8	-1																														
24	4	4	5	8	-2																													
30	7	14	6	3	5	-14																												
36	9	17	15	5	3	-5	-15																											
42	9	9	18	7	4	-3	-10	-17																										
48	6	10	9	11	2	0	-4	-14	-12																									
54	8	10	6	7	6	-5	-3	-6	-11	1																								
60	7	11	8	0	1	-6	-13	-8	-5	-4	4																							
66	11	8	5	4	-6	-4	-11	-12	-9	-1	2	8																						
72	6	10	3	3	-2	-13	-8	-13	-11	-6	3	8	6																					
78	5	9	9	2	-2	-8	-12	-10	-14	-4	-4	3	11	3																				
84	8	7	5	2	-4	-7	-13	-12	-11	-8	0	-3	1	6	-4																			
90	11	6	6	4	-1	-3	-6	-10	-3	-2	-1	5	1	-1	2	-6																		
96	6	3	2	8	1	-5	-5	-5	-6	0	-2	7	8	2	-3	-2	-4																	
102	0	-5	-10	-2	-2	-9	-9	-6	0	-2	4	6	14	10	5	-2	-5	-1																
108	-3	-9	-14	-9	-5	-5	-8	-6	2	2	6	8	6	13	8	7	-1	-8	-3															
114	3	-11	-16	-11	-14	-6	-7	-4	0	1	7	9	6	9	7	2	3	-1	-9	0														
120	-2	-10	-17	-11	-11	-6	-5	-6	2	1	7	6	6	8	5	0	-3	-2	-4	-9	-5													
126	-8	-7	-13	-7	-8	2	5	1	1	6	11	9	4	7	4	1	-6	-11	-9	-5	-9	-6												
132	-10	-7	-10	-10	-2	8	11	14	11	9	15	16	10	6	4	2	-4	-12	-13	-13	-10	-5	-6											
138	-14	-13	-11	-11	-12	7	11	18	22	13	14	15	12	11	5	-1	-3	-6	-11	-11	-15	-11	-5	-9										
144	-11	-18	-16	-7	-11	-1	12	16	20	20	16	14	8	11	10	3	-4	-3	-7	-8	-6	-14	-12	-4	-7									
150	-9	-11	-18	-8	-2	-1	4	13	13	14	13	9	7	4	3	4	-1	-7	-5	-4	1	-2	-5	-6	-2	1								
156	-11	-10	-10	-10	-4	4	1	7	9	6	4	2	3	3	-3	-4	0	-3	-7	-1	0	6	6	4	-2	0	4							
162	-12	-13	-8	-3	-4	5	4	7	16	5	-2	-4	-8	-1	0	-4	-10	-5	-3	-1	5	4	10	6	9	6	-2	7						
168	-8	-10	-7	-2	0	10	10	6	11	11	-3	-8	-18	-21	-8	-6	-11	-14	-9	1	5	4	5	7	4	12	6	-1	9					
174	-3	-4	-1	1	1	10	16	14	9	13	9	-5	-12	-18	-16	-10	-11	-6	-12	-4	4	8	3	5	3	1	5	5	-1	2				
180	0	-2	0	0	1	7	8	16	12	4	9	1	-9	-12	-16	-16	-13	-11	-9	-5	-3	5	7	1	1	-2	-5	1	5	1	4			
186	-1	-2	4	2	3	9	8	10	15	7	4	2	-7	-8	-6	-10	-5	-8	-9	1	3	2	2	5	-3	-3	-9	-8	-6	0	1	-6		
192	2	3	3	5	3	8	7	8	7	6	-1	-2	-5	-11	-2	1	6	9	2	3	9	14	6	3	3	-1	-4	-8	-5	-10	-1	2	-9	
198	1	5	6	2	1	3	2	3	1	-2	-6	-9	-7	-11	-12	1	8	13	17	9	9	16	17	7	-1	-2	0	-4	-6	-6	-9	-3	1	-12

noise. For Gaussian white noise, the contributions to the response from the two kernels $\{h_1, k_1, m_1, n_1\}$ and $\{h_2, k_2, m_2, n_2\}$ are weighted by factors $\alpha_1(=1/P_1)$ and $\alpha_2(=1/2P_1^2)$, respectively, where P is the power level of the Gaussian white input signal. However, since the earthquake excitation is nonwhite, the spectrum is not flat and it becomes difficult to characterize the entire spectrum through one number. This difficulty was circumvented in this analysis by using the following procedure to determine the relative weights of the linear and nonlinear kernels. The linear and nonlinear model responses over the entire input-output record were computed from the first-order kernels and second-order kernels with the weighting factors α_1 and α_2 as parameters (depending on P), and then these were chosen by a variational technique which minimized the mean-square error between the total (linear plus nonlinear) model response and the measured response. Admittedly, this procedure does not correct completely for the lack of whiteness in the input and only serves as a rough and partial compensation. As discussed in part I, the non-Gaussian (truncated distribution) nature of the signal does not lead to significant errors. However, the complete solution of the problem for such nonwhite, non-Gaussian inputs is being currently tackled.

Representative samples of the EW and NS model responses for the [3–43]-sec time windows are shown in Figures 6 and 7. Similar results were obtained for the [43–83]-sec time window, but they have not been shown here, for the main points in the discussion of the comparison between the model and the observed response are clearly brought out in these two figures.

We observe from these figures that the nonlinear contributions to the responses (Figures 6 and 7) are conparable in certain amplitude regions to the linear contributions. As we observed in part I, the linear part of the response is smaller than the observed response and is lacking in detail in that it does not have the high-frequency ripples that the actual response exhibits. These nonlinear contributions when added to the linear contribution improve the model responses quite appreciably. We notice that the nonlinear contribution dies down to a negligible value beyond about 9 sec in the NS direction and about 12 sec in the EW response. The effect of the addition of the nonlinear contribution was computed by using the integral of the square of the difference between the model responses and the measured responses as the error criterion. Together with the model responses computed for the two time windows obtained from the earthquake accelerograms, the model response obtained for an EW ambient vibration test, which was conducted in May 1973, was also computed. Normalizing the mean-square error of the zeroth order model to 100 units (i.e., the mean-square value of the response), we have the following reductions in the mean-square error for the sequence of models subjected to these inputs.

	Error				
	EW			NS	
Model	[3–43]	[43–83]	Ambient	[3–43]	[43–83]
h_0	100	100	100	100	100
$\{h_0, h_1\}$ linear	31	38	33	39	42
$\{h_0, h_1, h_2\}$ nonlinear	19	35	33	32	37

Discussion

The mean-square errors indicated above show that sizable reductions are obtained by the introduction of the nonlinear contributions to the response. It is noted that for the time windows [43–83] the percentage reduction in error caused by the inclusion of the nonlinear component is less than for the time windows [3–43], indicating the presence of a larger second-order nonlinearity in the latter time zone, both for the NS and EW

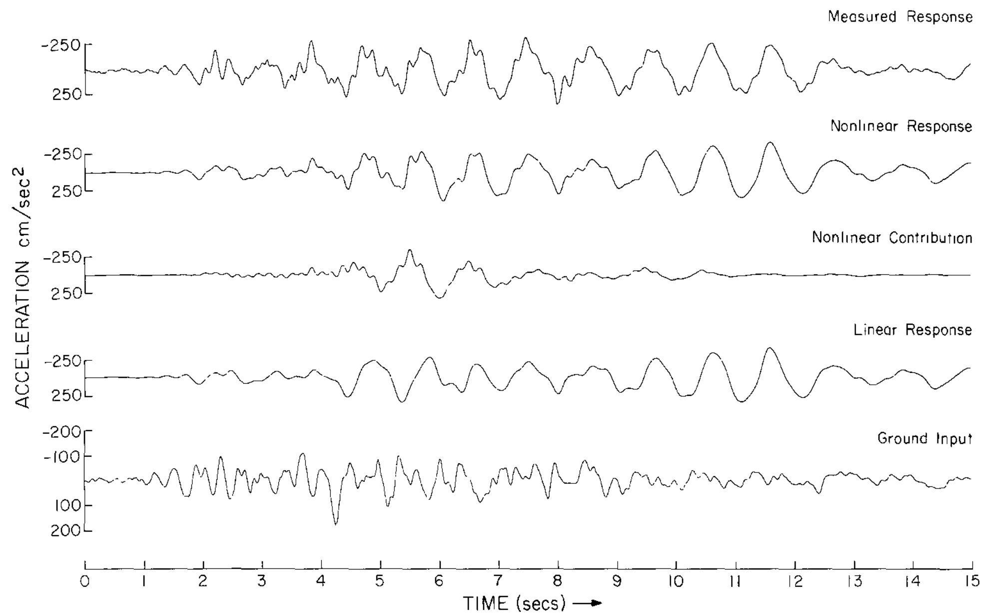

FIG. 6. Response analysis of Millikan Library EW component.

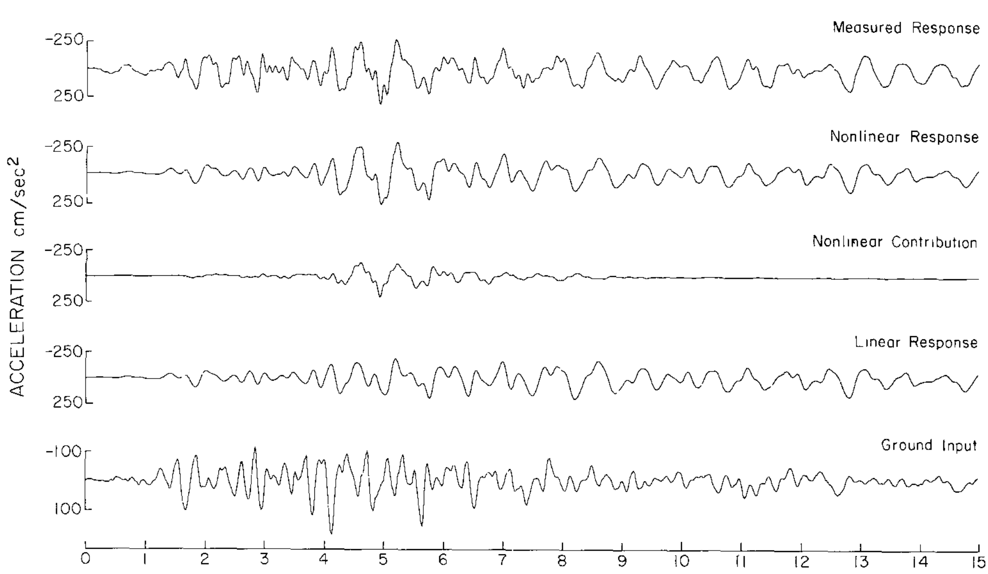

FIG. 7. Response analysis of Millikan Library NS component.

directions. Also it is observed that the linear model $\{h_0, h_1\}$ for the [43–83] time zone leads to larger mean-square errors. This has been attributed to two principal reasons: (a) the amplitudes of ground motion in this time zone are very small and the recovery of the data from the accelerograph trace causes the signal-to-noise ratio in the data to be low and (b) the forty-second length of data analyzed was not sufficiently long to eliminate statistical variances in the cross-correlations and smooth out the noise. The ambient data, although representing even lower amplitude ground motions, do not represent such a problem, for the time length of record available there was much longer leading to far greater error smoothing. We note that the extent of nonlinearity for the ambient data is negligible, there being no reduction in the mean-square error caused by the introduction of $G_2[h(t); x(\tau)]$.

As observed in part I, the cross-correlation scheme utilized requires a broadband flat input spectrum. The fact that the earthquake spectra are not exactly flat and reduce in amplitude beyond about 5 Hz (cf., part I) causes the linear model $\{h_0, h_1\}$ to be deficient in some of the higher-frequency content, thus causing an exclusion of some of them in the model response. Since it was argued that the second-order nonlinearity also introduces the higher-frequency ripples in the response, a logical question to ask would be, does the higher order nonlinearity $\{h_2\}$ put in these higher frequency ripples which in reality should have been introduced by the linear model, had its characterization been correctly done at the higher frequencies? As was discussed earlier, the two responses, $G_1[h_1(t); x(\tau)]$ and $G_2[h_2(t); x(\tau)]$ are orthogonal to each other for white-noise inputs, so that deficiencies in the linear model cannot be made good through the inclusion of any higher-order nonlinearity. This is indicated in Figure 6 where the ripples in the response around 14 Hz cannot be recovered from the model even with the inclusion of the second-order nonlinearity (although the second-order nonlinearity response clearly possesses such higher-frequency ripples). The fact then that the ripples cannot be correctly characterized by the model leads us to believe that they may be a consequence of a deficient linear model characterization (lacking in higher frequencies) or the consequence of higher order (>2) nonlinearities in operation.

The major difficulty in computing the high-order nonlinearities of a system is the long computation times on a digital computer required for the estimation of the higher-order cross-correlations required. The number of points for which each kernel argument is computed is m, where $m = \mu/\Delta t$ (μ is the system memory and Δt is the sampling interval). The nth order kernel must be estimated at $(n+m-1)!/n!(m-1)!$ points (taking into account the symmetry) and the total computation time required is given by

$$T_n = \alpha_n \cdot N \cdot n \cdot \frac{(m+n-1)(m+n-2)\ldots(m)}{n!}$$

where N is the total number of sample points in the record and α_n is a constant which accounts for the integration scheme used and for time spent in addressing, storing, etc. Thus, since computing time increases almost exponentially with the order of the kernel (if the cross-correlations are computed by conventional means, i.e., multiplication of the sampled data records), estimation of kernels of degree higher than the third take prohibitively long times even with the fastest digital machines currently available. However, several alternative avenues of kernel computation are open which could conceivably greatly alleviate this problem. Computation of the kernels by the use of the fast Fourier transform algorithm and recent hybrid computational methods are being currently investigated.

The digital machine used in this study had a core memory of 1 megabyte. Due to this storage limitation, the second-order kernels were computed for only 2 sec. Undoubtedly a better characterization (resulting in a much reduced model error) would have been possible had the duration of time for which it was computed been increased. To check the sensitivity of the values of $h_2(\tau_1, \tau_2)$ to the duration of time after which it was assumed zero, computations for a (1.1 sec times 1.1 sec) second matrix were performed.

The values obtained in both cases are very close to each other (within 1 per cent), showing that the function h_2 is relatively insensitive to the time length chosen. However, it must be emphasized that longer durations would lead to a better characterization of the second-order functional, thus improving the model responses considerably.

As noted, the applicability of the method is limited by the fact that the higher-order kernels are not easily computed. However, if the series is truncated after the nth order term, the resulting approximation to the system functional is the best nth order characterization in the mean-square-error sense. This, of course, is a direct result of the orthogonality of the terms of different degree in the Wiener series.

CONCLUSIONS

Wiener's general theory of nonlinear identification has been applied to the identification of a structural system from its input-output data obtained during an earthquake and during an ambient vibration test. Recorded earthquakes not only provide the large amplitude testing of a structure but, being broadband processes, also provide a high information rate about its input-output behavior over a given period of time as compared to testing with sinewaves. Before the method could be applied, the general zones where the system remained time-invariant were determined using a moving-window analysis technique. The memory of the system was estimated and the time durations for which the kernels needed to be estimated were determined. Here it was found that computer storage and time were two important factors to be considered. The first-order kernels were computed out to 10 sec for the earthquake data and up to 20 sec for the ambient data.

The first-order (linear) kernels computed showed that during the acceleration time history of ground motions the linear characteristics of the system changed quite drastically. The mean-square-error reduction of the linear model was found to be about 30 to 40 per cent, using the linear model obtained by direct cross-correlation methods.

The second-order kernels were computed out to only 2 sec due to limitations on computer storage. The values computed were found to be quite stable. The linear and nonlinear model responses were compared to the measured response. It was found that the inclusion of the second-order nonlinearity caused a significant improvement in the response prediction in the weaker EW direction. A comparison of the nonlinear kernels for each of the two time windows showed that the NS and EW kernels showed similar characteristics.

The effects of many types of contaminating noise sources (at the input, output or internally) are eliminated because of the orthogonality of the model series and the cross-correlation technique (statistical averages) used in estimating the kernels. This is evident from the analysis of the effect of noise on the kernel estimates as described in this study.

The method used in this paper has several assets. It clearly delineates the linear and nonlinear components of the response and provides a physical understanding of the amount of cross talk in the input caused by the nonlinearity. The method has a vast potential in determining the acceleration levels at which nonlinearities become significant and the nature of the various nonlinearities in different structures.

This paper represents the results of only a preliminary study of structural systems using the general technique. Such studies would have to be carried out on several structures and comparisons made of the extent and nature of nonlinearities in them.

An obvious extension of the method would be to colored inputs. Recent developments in virtual computer memory will make it possible to determine higher-order kernels, although such a study may become costly in computer time with the currently available algorithms.

REFERENCES

Wiener, N. (1958). *Nonlinear Problems in Random Theory*, Wiley, New York.

Bose, A. G. (1956), A theory of nonlinear systems, *Tech. Rept. 309*, Res. Lab. of Electronics, Mass. Inst. Tech., Cambridge, Mass.

Brilliant, M. B. (1958). Theory of the analysis of nonlinear systems, *Tech. Rept. 345*, Res. Lab. of Electronics, Mass. Inst. Tech., Cambridge, Mass.

George, D. A. (1958). Continuous nonlinear systems, *Tech. Rept. 355*, Res. Lab. of Electronics, Mass. Inst. Tech., Cambridge, Mass.

Lee, Y. W. and M. Schetzen (1965). Measurement of the kernels of a nonlinear system by cross-correlation, *Intern. J. Control* **2**, 237–254.

Marmarelis, P. Z. and K.-I. Naka (1974). Identification of multi-input biological systems, *IEEE Trans. Biomed. Eng.* **21**, 88–101.

Nielsen, N. N. (1966). Vibration test of a 9 story steel frame building, *J. Eng. Mech. Div., A.S.C.E.* **92,** 82–110.

Barrett, J. F. (1963). The use of functionals in the analysis of nonlinear physical systems, *J. Electron. Control* **15**, 567–615.

Marmarelis, P. Z. and K.-I. Naka (1973). Nonlinear analysis and synthesis of receptive-field responses in the catfish retina. I: Horizontal cell → ganglion cell chain, *J. Neurophysiol.* **36**, 605–618.

Udwadia, F. and P. Marmarelis (1975). The identification of building structural systems, I, The linear case, *Bull. Seism. Soc. Am.* **66**, 125–151.

Udwadia, F. E. and M. D. Trifunac (1975). Time and amplitude dependent response of structures, October, 1973.

CALIFORNIA INSTITUTE OF TECHNOLOGY
PASADENA, CALIFORNIA 91109

Manuscript received February 5, 1975.